Exploring the efficacy of RIPK3-rVACV infected CAR-T cells in solid tumors

Introduction

Cancer immunotherapy is one of the most promising strategies to overcome cancer, especially chimeric antigen receptor (CAR) T cell immunotherapy, which has shown overwhelming success in hematopoietic tumors while limited efficacy in solid tumors (June et al., 2018; Labanieh et al., 2018; Newick et al., 2017). Oncolytic viral therapy, the other effective cancer therapy, can induce local and systemic specific anti-tumor immunity (Lin et al., 2023), but is limited to the tumor tropism, insufficient proinflammatory cytokine production and high patient burden (Jin et al., 2021). Combined immunotherapies are the hot topics currently due to their achieved complementary advantages. A previous study reported that a novel immunotherapy combining anti-CD19 CAR-T with recombinant vaccinia virus (rVACV) delivering truncated CD19 into tumor cells can eliminate the tumor antigenic heterogeneity, meanwhile, the introduction of the oncolytic virus reversed the malignant tumor microenvironment (Park et al., 2020). A later study reported the combination of CAR-T and myxoma virus could induce the autosis of tumor cells and reinforce tumor clearance (Zheng et al., 2022). These study shows the promising clinical applications of CAR-T + Oncolytic virus therapy. It's very curious that whether introducing a gene into both tumor cells and CAR-T cells through oncolytic virus, which can induce inflammatory cell death in tumor cells and enhance T-cell immunity, will lead to an unexpectedly rapid tumor clearance. This study therefore aims to develop a therapy that enhances both CAR-T efficacy and cancer-related inflammatory death through rVACV.

Graphical design

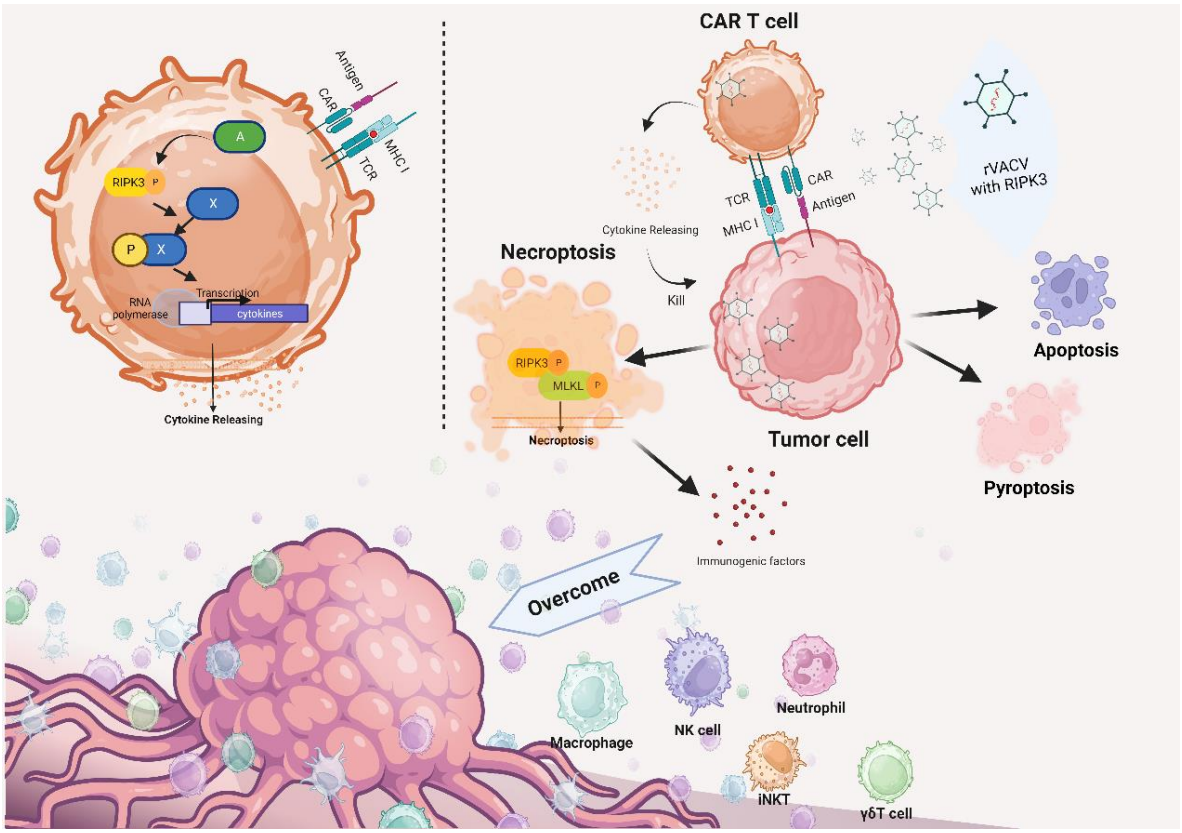

Progress

1. **RIPK3 is a promising target, which is crucial in necroptosis and positively associated with T cell immunity.**

Necroptosis is significant in health and disease because it differs from other forms of cell death, particularly apoptosis, by being highly proinflammatory due to the loss of cell membrane integrity, thus triggering immune system activation and inflammation (Cho et al., 2009). Receptor-interacting protein kinase-3 (RIPK3, or RIP3) is an essential protein of necrosome, which initiates programmed necrotic cell death called necroptosis (Chan et al., 2015). Previously, a necroptosis-independent function of RIPK3 in NF-κB activation, dendritic cells biology, innate inflammatory-cytokine expression was illustrated (Moriwaki et al., 2014). Considering the crucial role of NF-κB activation in immunology, RIPK3 may also have necroptosis-independent function in other immune cells, especially in T cells. Recent two independent studies reported the RIPK3 causes CD4 T cell senescence through activating mTOR pathway (Imanishi et al., 2023) and evokes a dysregulated type 1 interferon response, which was linked to an impaired antiviral immune response, respectively (Preston et al., 2023). Also, in natural killer T cells, RIPK3 was evidenced to interact with PGAM5 and had a significant role in regulating NFAT signaling and mitochondrial function (Kang et al., 2015). Thus, its necroptosis-independent role of T cells seems to be pro-inflammatory which may develop as a promising target for synthetic T cell immunotherapy. Delivering RIPK3 by effective media has the potential to enhance T cell immunotherapy at the same time to promote oncolytic immune responses, which could result in a valid efficacy in solid tumors. Pyroptosis, also known as inflammatory necrosis, is another programmed proinflammatory cell death taken into consideration. Its hallmark is the phenomenon where tumor cells, under the influence of drugs, exhibit characteristics such as membrane pore formation, cell swelling, and dissolution (Yu et al., 2021). This leads to the release of inflammatory factors and cellular contents, triggering a robust inflammatory response, activating anti-tumor immunogenicity, and suppressing tumor growth and metastasis (Bergsbaken et al., 2009; Burdette et al., 2021). GSDMD is a crucial gene in Pyroptosis, and its deficiency reduced the cytolytic capacity of $CD8^+$ T cells (Xi et al., 2019). Considering Pyroptosis and Necroptosis are two classical inflammatory cell death, GSDMD (Burdette et al., 2021; Shi et al., 2015), and RIPK3 (Chan et al., 2015; Cho et al., 2009) are firstly compared through Pan-cancer analysis. Firstly, tumor immune infiltration analysis with CD8+ T cells on RIPK3 and GSDMD were performed based on TIMER (Li et al., 2016; Li et al., 2017). The expressions of both RIPK3 and GSDMD are demonstrated to be positively correlated with CD8+ T cell infiltration (Fig.1A). Notably, RIPK3 is more positively correlated in DLBC (Diffuse Large B-cell Lymphoma), a B-cell solid tumor currently treated with anti-CD19 CAR-T clinically (Fig.1A). To further understand the role of RIPK3 and GSDMD, panGTBA analysis (https://guotosky.vip:13838/GTBA/) based on KEGG gene sets (https://www.genome.jp/kegg/) and TCGA tumor datasets (https://www.cancer.gov/tcga) were performed (Fig.1B, C, G). Obviously, the expression of RIPK3 is more positively correlated with many immune-related pathways, especially the T cell receptor signaling pathway, whose activation is positively correlated with RIPK3 expression in most cancers (Fig.1B, E, F, H, I), but not enriched in the panGTBA analysis of GSDMD (Fig.1C, S1). The immune infiltration analysis based on MCPcounter was further used to visualize the relationship between RIPK3 and immune cell infiltrations (Becht et al., 2016). Thus, RIPK3 was identified as a promising target for oncolytic viral delivery.

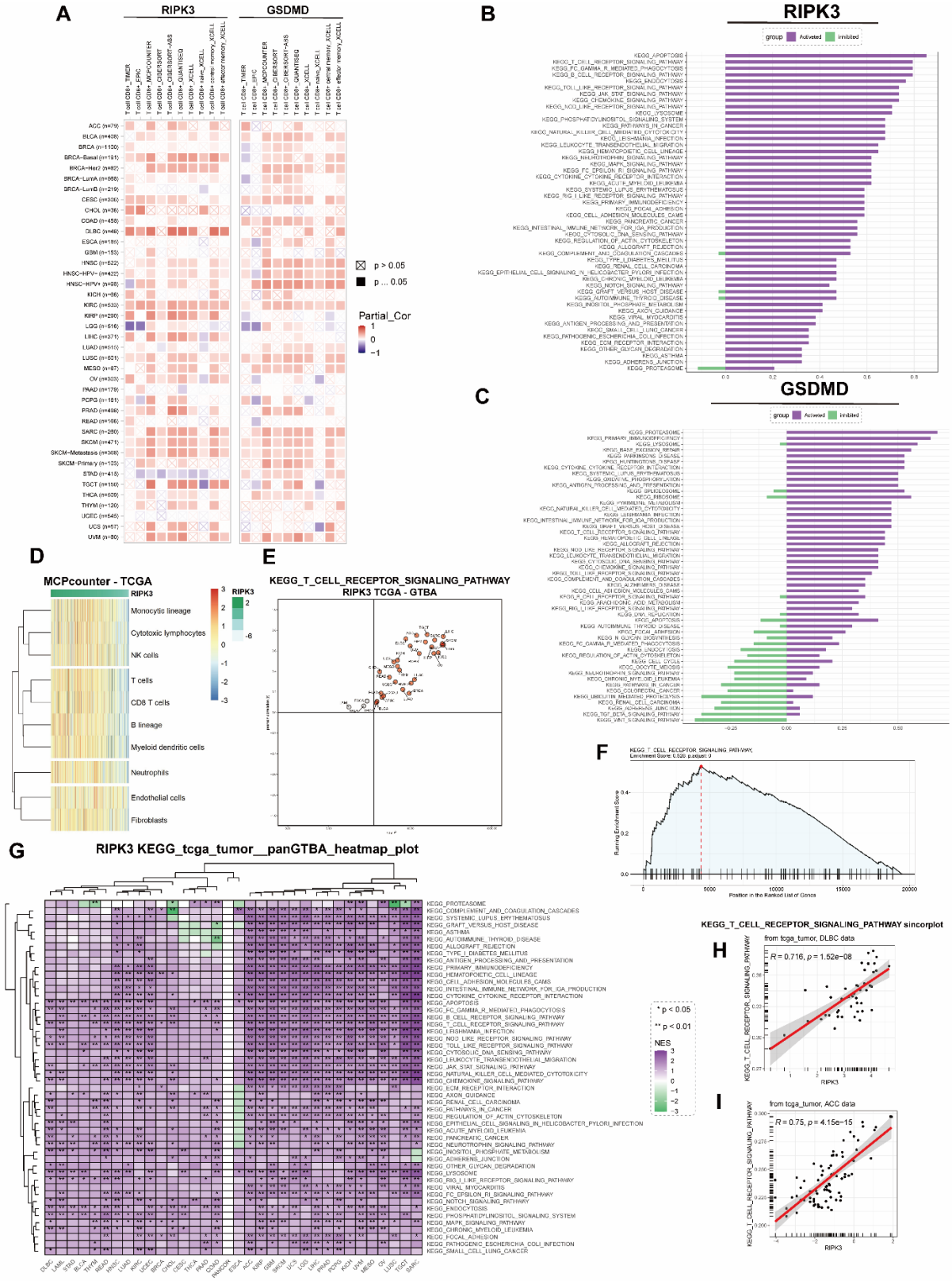

Fig.1| Pan-cancer comparison between RIPK3 and GSDMD. A. CD8+ T cell-related infiltrating analysis of RIPK3 and GSDMD. B, C. Pan-cancer KEGG analysis of RIPK3 and GSDMD. D. MCPcounter-based immune infiltrating analysis of RIPK3. E, F. KEGG visualization of enriched KEGG T cell receptor signaling pathway in pan-cancer analysis. G. KEGG pathway enrichment and protein expression analysis of RIPK3.

2. RIPK3 is dynamically changed during T cell development and correlated with pro-inflammatory cytokines.

The expression of RIPK3 in T cells is further explored and central memory T cells (TCM) and effector memroy T cells (TEM) have a higher RIPK3 expression than naïve T cells (TNaiveLike) (Fig.1C, D, S3). The phenomena has been illustrated in murine naïve and effector/memory T cell (Imanishi et al., 2023). Exhausted CD8 T cells (CD8.TEX) and Regulary T cells (CD4.Treg) have the highest expression of RIPK3, but no studies focus on the function of highest RIPK3 expression in exhausted CD8 T and Tregs (Fig. 2A,B). It's worthy noting that the expression percentage of RIPK3 is rellay low in single-cell RNA sequencing datasets so ImmuNexUT (RNAseq datasets) was used to validate the phenomena (Fig.S4) (Ota et al., 2021). A previous study reported in murine T cells, the released TNF-α, IFN-γ and IL-4 by activated T cells were not affected by Ripk3 (Kang et al., 2015). To further explore the role of RIPK3 in T cell activation, the differential expressed genes (DEGs) were found and shown in Fig.8. IFNG, TNF, GZMB, NFKB1, TIGIT, NFKBIB, NFATC3, GZMM, CD28, SELL, TOX, LAG3 were found in human tumor infiltrating lymphocytes (TIL) atlas (Fig.2C, Table S1) while Nfkb1, Nfkb2, Cd69, Tox4 were found in mouse TIL atlas (Table S2). Especially, IFNG is significantly correlated with RIPK3 in CD8.TEM. Based on a study about CRISPR activation (CRISPRa) and interference (CRISPRi) screens in primary human T cells, the CRISPRa on RIPK3 in primary CD4 T cells significantly increases the releasing of IL2 and IFNG, while CRISPRi shows on obvious effect (Fig.S1) (Schmidt et al., 2022). These results indicate a RIPK3-denpendent pro-inflammatory pathway contributes to T cell killing efficiency in T cells, which is unnecessary for T cell activation and proliferation (further GSEA/GSVA pathway analysis should be finished).

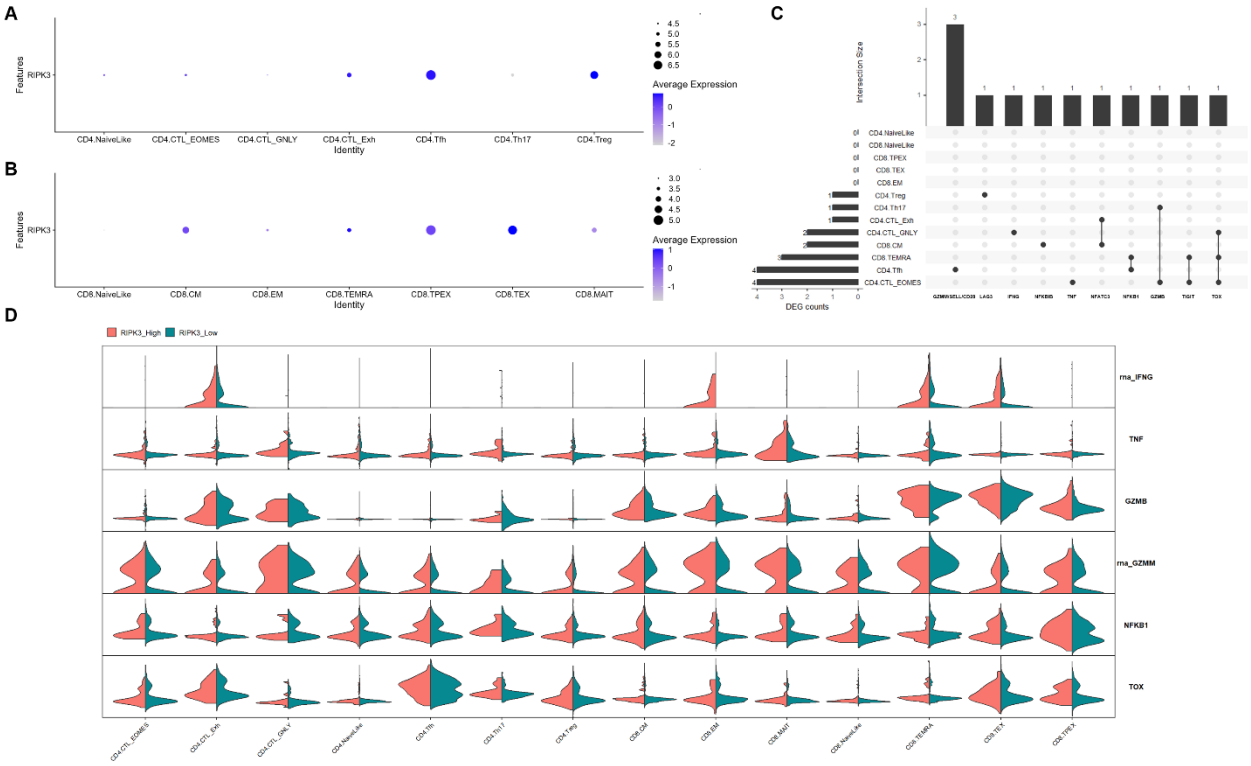

Fig.2| The gene expression of RIPK3 in T cells and its correlation with cytokines. A, B. The mRNA levels of RIPK3 in different CD4 T cell, CD8-T cell subtypes.

3. Inhibit RIPK3 kinase activity slightly inhibit the CAR-T killing efficiency.

Consider RIPK3 as a kinase, its role in T cell may depend on phosphorylation, so GSK872 (RIPK3 specific kinase inhibitor) was added in T cell activation ex vivo. PD-1 (data not shown), CD4, CD8 was detected after 5 days and GSK872 shows no significant toxicity and impact on the T cell activation and CD4:CD8 ratio (Fig.3A) (time is truly short). While a previous genome wide CRISPR screens in primary human T cells reveal RIPK3 as a key negative regulator for CD8 T cell proliferation (Fig.6) (Shifrut et al., 2018). Thus, RIPK3 may have a T-cell based common role in T cell proliferation and activation, like in activation-induced cell death (AICD). Further studies are in need to detect the RIPK3 phosphorylation during T cell activation and the impact of GSK872 on T cell proliferation and AICD. As mentioned above, RIPK3 has an impact on the released cytokines of T cell, which also illustrates its role on T cell killing efficiency. To further explore the role of RIPK3 in T cell activation, anti-CD19-BBz chimeric antigen receptor (CAR, CAR19)-T cells were produced to examine the influence of GSK872 on T cell killing activity. Nalm6, a human B lymphoblastic leukemia cell line with high expression of CD19 and no expression of RIPK3 was selected as target cell line. The results show GSK972 has an inhibitory function on CAR-T cells (Fig.3B, C) (quantitative assay is currently not stable, needs to repeat and adjust). Notably, GSK872 is a RIPK3 kinase inhibitor, it only can show necroptosis/ kinase dependent role of RIPK3 but not kinase independent role in T cells.

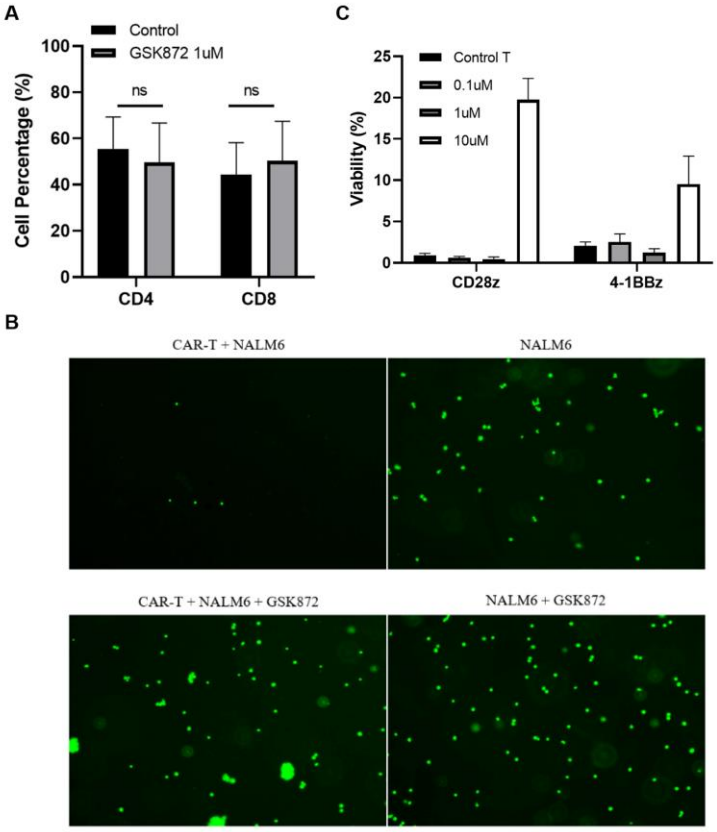

Fig.3|A. The CD4/CD8 T cell percentage after 5 days activation with/without GSK872. Replicated for 3 times/samples from three people. Activated for 5d with anti-CD3 micro-beads (Genscript), 96-well plate. APC anti-CD4 (Biolegend), PE anti-CD8b (Biolegend), FITC anti-CD279/PD-1 (Invitrogen). B. Fluorescent photos of Nalm6 after 48h CAR-T (BBz) killing (E: T = 4:1). C. Quantification of targeted cell (Nalm6) activity through luciferase after 24h CAR-T (both 28z and BBz) killing.

Next plan

1. Further analyze the RIPK3-IFNG axis and its role of RIPK3 in T cell immunity based on the single cell datasets.
2. Delete RIPK3 in Jurkat cells and examine the cytokine-relevant RNA (mainly the genes enriched by single cell-datasets based DEGs like IFNG) changes after T cell activation. If no obvious changes, primary T cells will be considered to repeat the experiments.
3. Expand rVACV-RIPK3 and infect Jurkat and primary T cells, then examine the cytokine-relevant RNA changes after T cell activation. (As the transduction of RIPK3 in CAR-T cells is really difficult because the dual-transduction by lenti-virus will decrease the T cell activity. At the same time, the overview design of the study doesn't focus on the overexpression of RIPK3 on T cells currently, and the overexpression of RIPK3 seems to severely influence cell viability. I focus more on could rVACV-RIPK3 enhance the CAR-T efficiency currently, so using currently available rVACV-RIPK3 is relatively easier to deliver RIPK3 into T cells within a low percentage. The best percentage of infected cells will be further tested to realize the best viral delivery and T cell enhancement.) How to generate rVACV-RIPK3 has been described in detail (Liu et al., 2021). The relevant methods are described in the next section.
4. Apply rVACV-RIPK3 in CAR-T killing systems and examine whether the rVACV could enhance the killing efficiency. If the rVACV could enhance CAR-T efficiency as expected, further experiments will focus on the detailed mechanisms.

Methods

Virus expansion

The rVACV with or without RIPK3 has been generated by Dr. Zhijun Liu. The viruses will be passaged in BS-C-1 cells by infection at MOI = 0.1. After 72 hours, cells will be harvested by washing in 1X PBS twice. The resulting pellets will be resuspended in PBS supplemented with 0.1% bovine serum albumin. The suspensions will be subjected to 3 cycles of freeze and thaw.

Viral titer determination

Serial 10-fold dilutions were made for the viral titers will be determined by plaque assays on Vero cells. After 2 days of infection, Vero cells will be fixed in 5% formaldehyde for 30 minutes, followed by staining with 0.1% crystal violet in 1% formalin. After rinsing with water, plaques will be counted by eye.

Virus infection in cell culture

The Jurkat and primary T cells will be infected with the indicated viruses at MOI = 2 firstly. Then a fit MOI will be explored with a viral MOI titration. Cells are all incubated with virus in RPMI 1640 (Thermo Fisher) supplemented with 2.5% fetal calf serum for 2 hours before changing to medium with 10% fetal bovine serum. Twelve hours after infection, the infected T cells will be used for next experiments, such as co-killing model, WB and so on.

Cell lines

HEK293T cells were provided by Prof. Francis Chan (Zhejiang University) and were maintained in DMEM (Gibco) supplemented with 10% FBS (Thermo Fisher). Jurkat T cell line and Nalm-6 cell line expressing GFP and luciferase were gifts from Dr. Xin Jin and Prof. He Huang (Zhejiang

University) and were maintained in RPMI-1640 (Thermo Fisher) supplemented with 10% FBS (Thermo Fisher).

Isolation and expansion of human primary T cells

Fresh peripheral blood mononuclear cells (PBMCs) from healthy donors were provided by the First Affiliated Hospital, College of Medicine, Zhejiang University. PBMCs were isolated by density gradient centrifugation using Ficoll (Sigma-Aldrich). T cells were activated through anti-CD3 microbeads (Genescript), and cultured T cells were cultured in Roswell Park Memorial Institute (RPMI) 1640 medium (Thermo Fisher) and recombinant human IL-2 (100 U ml^{-1}). Cells were collected once cell number reached the requirement for administration and then washed, formulated and cryopreserved.

CAR-T cell generation by lentivirus

The CAR sequence was cloned into the pCDH lentiviral vector backbone containing an EF1α promoter. Lentivirus was produced by transfecting 293T cells with anti-CD19(FMC63)-4-1BB-CD3z-mCherry CAR plasmid, pMD2.G and psPAX2 using Lipofectamine 3000 (Thermo Fisher). Virus-containing supernatants were collected after 3 d to infect primary human T cells after stimulating for 3 d and transduced efficiency was checked by flow cytometry.

Luciferase examination

D-Luciferin 10uM was added into 96 well-plates. The whole 96 well-plate was maintained at 37°C for around 10 minutes and then the fluorescence intensity was examined by BioTek Synergy2 Multimode Enzyme-labelled instrument and analyzed by Gen5.

Western blot

Cell lysates were prepared using RIPA lysis buffer (25 mM Tris-HCl, 150 mM NaCl, 0.5 mM EDTA, 0.1% SDS, 0.5% Sodium deoxycholate) supplemented with 1X *Complete* protease inhibitor cocktail (Roche) and 1X phosphatase inhibitor cocktail (Sigma). Insoluble material was removed via centrifugation at 15,000 rpm for 15 minutes at 4°C. Soluble lysates were transferred to new Eppendorf tubes. Protein concentrations were determined with the BCA Protein Assay (ThermoFisher). The gel was transferred to nitrocellulose membrane using the Bio-Rad Trans-Blot Turbo system. The antibody used are listed below. Clarity or Clarity Max ECL western blotting substrates were used for chemiluminescence detection. Chemiluminescence signals were detected using the ChemiDoc MP System from Bio-Rad. Antibodies for western blot used in the study include: hRIPK3 (Santa Cruz #sc-374639), β-actin (CST Bioscience #3700S).

Fluorescence microscopy

The relevant cells were put into 48/96-well plate and then taken photos with Leica THUNDER Imager Live Cell. All the generated photos were processed through Leica Application Suite X (LAS X).

Flow cytometry

CAR and membrane protein expression was determined by flow cytometry. Cells were prewashed and incubated with antibodies for 30 min on ice away from light. After washing twice, samples

were run on an LSRFortessa (BD Biosciences) and analyzed with FlowJo software. The following antibodies were used: FITC anti-human CD3, APC anti-human CD4, PE anti-human CD8b, APC anti-human CD69 (all from BioLegend), FITC anti-human CD279 (Thermo Fisher). For detection of CAR expression, PC5.5 channel was used to detect mCherry. The percentage of CAR^+ cells was analysed in mCherry+ gated cells.

Information of single-cell transcriptome data

GSE186596 was downloaded from the Gene Expression Omnibus (GEO) database (http://www.ncbi.nlm.nih.gov/geo), ProjecTILs (https://github.com/carmonalab/ProjecTILs) and the Open Targets website (https://www.opentargets.org/projects/effectorness).

Differential expression and functional enrichment analysis of DEGs

To overview transcriptional differences between RIPK3+ and RIPK3- cells, DEGs were calculated by the package DESeq2 or limma. PCA plots were not performed. Furthermore, the functional enrichment for RIPK3+ T cells was assessed using enrichKEGG and GSEA in R package clusterProfiler. The heatmaps of main up-regulated and down-regulated genes in the above significant enriched pathways (p-value cutoff < 0.05) were shown via ggplot2. Moreover, to probe into the features and function of each cluster, functional enrichment was performed in the same way mentioned above.

Data filtration, integration, analysis and visualization of cells

R package Seurat (version 4.1.2) was performed for subsequent analysis. EnrichKEGG function from clusterProfiler was performed for functional pathway analysis. R packages for visualization used in the study include: ggplot2, scCustomize, dittoSeq, ggunchained, ggpubr, Upset.

Information of public transcriptome and proteome datasets

GSE16792, GSE109161, GSE231310, GSE151774, GSE212072 were downloaded from the Gene Expression Omnibus (GEO) database (http://www.ncbi.nlm.nih.gov/geo). PXD015315 was downloaded from the Proteomics Identifications (PRIDE) database (https://www.ebi.ac.uk/pride/). The data for human organ proteomics data was derived from Jiang et al., 2020 and downloaded from the table s2 and s3 in supplemental information at doi.org/10.1016/j.cell.2020.08.036 (Jiang et al., 2020). The figures from HPA, GTEx, ImmuNexUT are downloaded from https://www.proteinatlas.org/ENSG00000129465-RIPK3/single+cell+type, https://www.gtexportal.org/home/gene/RIPK3, https://www.immunexut.org/eqtlGenes?gene_symbol=RIPK3, respectively.

Code availability

No original code was generated. All the relevant tools and used packages were illustrated above. All the used tools were mentioned in the Progress and Methods sections. Other codes for generating figures can be found at https://github.com/ChentaoLi.

Supplementary information

Fig.S1| KEGG pathway enrichment and protein expression analysis of GSDMD.

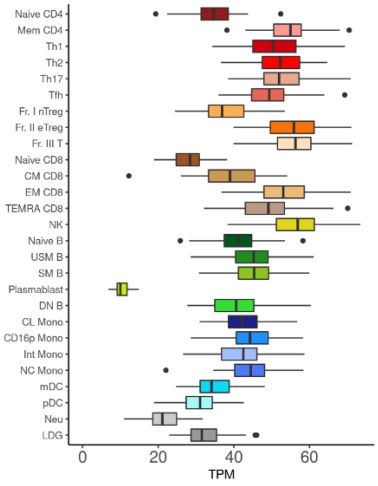

Fig.S2| The mRNA level of RIPK3 in peripheral immune cells.

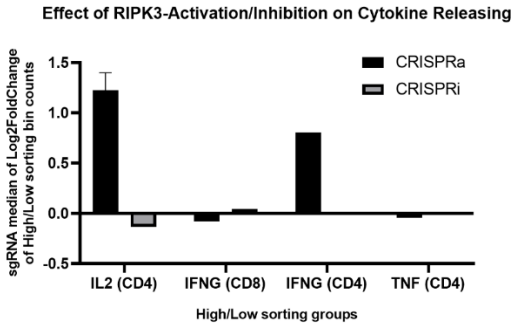

Fig.S3| Effect of RIPK3 activation and inhibition on the cytokine releasing of T cells.

References

Becht, E., Giraldo, N.A., Lacroix, L., Buttard, B., Elarouci, N., Petitprez, F., Selves, J., Laurent-Puig, P., Sautès-Fridman, C., Fridman, W.H., *et al.* (2016). Estimating the population abundance of tissue-infiltrating immune and stromal cell populations using gene expression. Genome Biol *17*, 218.

Bergsbaken, T., Fink, S.L., and Cookson, B.T. (2009). Pyroptosis: host cell death and inflammation. Nat Rev Microbiol *7*, 99-109.

Burdette, B.E., Esparza, A.N., Zhu, H., and Wang, S. (2021). Gasdermin D in pyroptosis. Acta Pharm Sin B *11*, 2768-2782.

Chan, F.K., Luz, N.F., and Moriwaki, K. (2015). Programmed necrosis in the cross talk of cell death and inflammation. Annu Rev Immunol *33*, 79-106.

Cho, Y.S., Challa, S., Moquin, D., Genga, R., Ray, T.D., Guildford, M., and Chan, F.K. (2009). Phosphorylation-driven assembly of the RIP1-RIP3 complex regulates programmed necrosis and virus-induced inflammation. Cell *137*, 1112-1123.

Imanishi, T., Unno, M., Yoneda, N., Motomura, Y., Mochizuki, M., Sasaki, T., Pasparakis, M., and Saito, T. (2023). RIPK1 blocks T cell senescence mediated by RIPK3 and caspase-8. Sci Adv *9*, eadd6097.

Jiang, L., Wang, M., Lin, S., Jian, R., Li, X., Chan, J., Dong, G., Fang, H., Robinson, A.E., and Snyder, M.P. (2020). A Quantitative Proteome Map of the Human Body. Cell *183*, 269-283.e219.

Jin, K.T., Du, W.L., Liu, Y.Y., Lan, H.R., Si, J.X., and Mou, X.Z. (2021). Oncolytic Virotherapy in Solid Tumors: The Challenges and Achievements. Cancers (Basel) *13*.

June, C.H., O'Connor, R.S., Kawalekar, O.U., Ghassemi, S., and Milone, M.C. (2018). CAR T cell immunotherapy for human cancer. Science *359*, 1361-1365.

Kang, Y.J., Bang, B.R., Han, K.H., Hong, L., Shim, E.J., Ma, J., Lerner, R.A., and Otsuka, M. (2015). Regulation of NKT cell-mediated immune responses to tumours and liver inflammation by mitochondrial PGAM5-Drp1 signalling. Nat Commun *6*, 8371.

Labanieh, L., Majzner, R.G., and Mackall, C.L. (2018). Programming CAR-T cells to kill cancer. Nat Biomed Eng *2*, 377-391.

Li, B., Severson, E., Pignon, J.C., Zhao, H., Li, T., Novak, J., Jiang, P., Shen, H., Aster, J.C., Rodig, S., *et al.* (2016). Comprehensive analyses of tumor immunity: implications for cancer immunotherapy. Genome Biol *17*, 174.

Li, T., Fan, J., Wang, B., Traugh, N., Chen, Q., Liu, J.S., Li, B., and Liu, X.S. (2017). TIMER: A Web Server for Comprehensive Analysis of Tumor-Infiltrating Immune Cells. Cancer Res *77*, e108-e110.

Lin, D., Shen, Y., and Liang, T. (2023). Oncolytic virotherapy: basic principles, recent advances and future directions. Signal Transduct Target Ther *8*, 156.

Liu, Z., Kang, K., and Ka-Ming Chan, F. (2021). Generation of recombinant vaccinia virus and analysis of virus-induced cell death. STAR Protoc *2*, 100871.

Moriwaki, K., Balaji, S., McQuade, T., Malhotra, N., Kang, J., and Chan, F.K. (2014). The necroptosis adaptor RIPK3 promotes injury-induced cytokine expression and tissue repair. Immunity *41*, 567-578.

Newick, K., O'Brien, S., Moon, E., and Albelda, S.M. (2017). CAR T Cell Therapy for Solid Tumors. Annu Rev Med *68*, 139-152.

Ota, M., Nagafuchi, Y., Hatano, H., Ishigaki, K., Terao, C., Takeshima, Y., Yanaoka, H., Kobayashi, S., Okubo, M., Shirai, H., *et al.* (2021). Dynamic landscape of immune cell-specific gene regulation in immune-mediated diseases. Cell *184*, 3006-3021.e3017.

Park, A.K., Fong, Y., Kim, S.I., Yang, J., Murad, J.P., Lu, J., Jeang, B., Chang, W.C., Chen, N.G., Thomas, S.H., *et al.* (2020). Effective combination immunotherapy using oncolytic viruses to deliver CAR targets to solid tumors. Sci Transl Med *12*.

Preston, S.P., Allison, C.C., Schaefer, J., Clow, W., Bader, S.M., Collard, S., Forsyth, W.O., Clark, M.P., Garnham, A.L., Li-Wai-Suen, C.S.N., *et al.* (2023). A necroptosis-independent function of RIPK3 promotes immune dysfunction and prevents control of chronic LCMV infection. Cell Death Dis *14*, 123.

Schmidt, R., Steinhart, Z., Layeghi, M., Freimer, J.W., Bueno, R., Nguyen, V.Q., Blaeschke, F., Ye, C.J., and Marson, A. (2022). CRISPR activation and interference screens decode stimulation responses in primary human T cells. Science *375*, eabj4008.

Shi, J., Zhao, Y., Wang, K., Shi, X., Wang, Y., Huang, H., Zhuang, Y., Cai, T., Wang, F., and Shao, F. (2015). Cleavage of GSDMD by inflammatory caspases determines pyroptotic cell death. Nature *526*, 660-665.

Shifrut, E., Carnevale, J., Tobin, V., Roth, T.L., Woo, J.M., Bui, C.T., Li, P.J., Diolaiti, M.E., Ashworth, A., and Marson, A. (2018).

Genome-wide CRISPR Screens in Primary Human T Cells Reveal Key Regulators of Immune Function. Cell *175*, 1958-1971.e1915.

Xi, G., Gao, J., Wan, B., Zhan, P., Xu, W., Lv, T., and Song, Y. (2019). GSDMD is required for effector CD8(+) T cell responses to lung cancer cells. Int Immunopharmacol *74*, 105713.

Yu, P., Zhang, X., Liu, N., Tang, L., Peng, C., and Chen, X. (2021). Pyroptosis: mechanisms and diseases. Signal Transduct Target Ther *6*, 128.

Zheng, N., Fang, J., Xue, G., Wang, Z., Li, X., Zhou, M., Jin, G., Rahman, M.M., McFadden, G., and Lu, Y. (2022). Induction of tumor cell autosis by myxoma virus-infected CAR-T and TCR-T cells to overcome primary and acquired resistance. Cancer Cell *40*, 973-985.e977.